



Development of Heating Technologies for the  
Efficient Renewable Energy Consumption of  
CO<sub>2</sub>-Neutral Downstream-Processes

## **Deliverable 2.1**

### *Short-term heat recovery analysis*

Piero Frittella (FER), Tommaso Grossi (SSSA), Ismael Matino (SSSA), Valentina Colla (SSSA), Oliver Hatzfeld (BFI), Antonio Curci (ADI), Wolfgang Adler (BFI), Benedict Philippi (BFI)

March 16<sup>th</sup>, 2026

*This project has received funding from the European Union under grant agreement NUMBER — **101178210** — E-ECO Downstream*

*The information and views set out in this document do not necessarily reflect the official opinion of the European Commission. The European Commission does not guarantee the accuracy of the data included in this document. Neither the European Commission nor any person acting on the European Commission's behalf may be held responsible for the use which may be made of the information contained therein.*

## Table of content

<b>1. Summary</b> .....	4
<b>2. Thermal mapping of industrial sites</b> .....	5
2.1 Feralpi Siderurgica Site Analysis .....	5
Steelmaking Area .....	5
Rolling Area .....	5
Main Sources Considered in the E-ECO-Downstream Project.....	6
Summary .....	6
2.2 Acciaierie d'Italia Site Analysis.....	10
Heat losses during hot rolling .....	10
Heat losses of coils from the down coiler to the storage .....	12
Heat loss from the skid beam cooling.....	15
<b>3. Theoretical Framework for Heat Recovery</b> .....	16
3.1 Thermodynamic principles for waste heat recovery .....	16
Implications for Source Selection .....	19
3.2 Heat recovery technologies overview .....	19
3.3 Preheating strategies.....	20
Fuel preheating .....	20
Oxidizer (air/oxygen-enriched) preheating .....	20
Mixed strategies .....	21
3.4 Compatibility with future fuels (H <sub>2</sub> , biofuels) .....	21
Hydrogen Combustion Characteristics .....	21
Material Compatibility for Hydrogen Combustion.....	22
Biofuel compatibility.....	22
<b>4. Selection and Prioritization of Heat Sources</b> .....	23
4.1 Selection Methodology .....	23

---

4.2 Feralpi Siderurgica Priority Sources .....	23
Priority 1: EAF Off-Gas Before Quenching .....	24
Priority 2: Roll Mill 2 Off-Gas from Billet Preheating .....	26
Priority 3: EAF Off-Gas After Quenching .....	28
Non-Prioritized Sources: EAF Secondary Off-Gas .....	29
Priority 4: Preheating of combustion fuel with EAF Off-gas .....	30
Priority 5: Heat pumps for warm water provision of local facilities .....	31
Summary of Priority Ranking.....	32
4.3 Acciaierie d'Italia Priority Sources.....	33
Priority 1: Heat losses during hot rolling .....	33
Priority 2: Radiant heat from coil cooling (down coiler to storage).....	34
Priority 3: Skid beam cooling systems.....	35
Summary of Priority Ranking.....	36
<b>5. Conclusions and recommendations .....</b>	<b>37</b>

## 1. Summary

In steel production, the high levels of heat and energy consumption also result in significant residual energy losses.

In general, the amount of recoverable residual energy is linked to the potential for energy recovery, but this is not always feasible due to variations in the characteristics of the available energy — for example, cases of high temperature with low flow, or high flow with very low temperature.

Furthermore, this residual energy can exist in different forms or media, such as off-gases, water, or radiant heat released into the atmosphere.

For this purpose, the present item covers the following aspects:

- Conducting a thermal mapping of residual energy sources;
- Evaluating possible recovery methods;
- Studying technologies or systems capable of recovering such energy;
- Defining the characteristics of potential users who can utilize the recovered energy;
- Developing feasibility analyses to assess the potential benefits and implementation opportunities.

Based on these analyses, an internal decision will be made to identify the best recovery cases.

Initially, industrial partners carried out the thermal mapping of the residual energy available at the industrial sites.

## 2. Thermal mapping of industrial sites

### 2.1 Feralpi Siderurgica Site Analysis

Following the thermal mapping activities carried out at the **Feralpi Siderurgica** site, the plant can be divided into two main operational areas:

- **Steelmaking Area**
- **Rolling Area**

#### Steelmaking Area

Within the steelmaking section, several potential sources of residual energy have been identified:

1. **Off-gas from the Electric Arc Furnace (EAF) primary duct**, subdivided into:
  - 1.1. **At the 4th hole position**
  - 1.2. **Upstream of the quenching tower**
  - 1.3. **Downstream of the quenching tower**
2. **Off-gas from the EAF secondary duct**
3. **Hot air from ladle preheating** (two stations)
4. **Hot air from tundish drying**
5. **Hot water from EAF cooling systems** (roof, shell, and off-gas duct)
6. **Hot water from auxiliary cooling systems**
7. **Radiant heat emitted by hot billets**

#### Rolling Area

In the rolling section, the following sources of recoverable energy have been identified:

8. **Off-gas from the reheating furnace**, subdivided into:
  - 8.1. **Upstream of the thermal recuperator**
  - 8.2. **Downstream of the thermal recuperator**
9. **Radiant heat from rebars and wire rods**

## Main Sources Considered in the E-ECO-Downstream Project

Based on the analysis of thermal data from the different media, the **E-ECO Downstream project** has focused on the following key sources for residual energy:

- **Off-gas from the EAF primary duct**, specifically:
  - Upstream of the quenching tower
  - Downstream of the quenching tower
- **Hot air from ladle preheating** (two stations)
- **Hot air from tundish drying**
- **Off-gas from the reheating furnace** (downstream of the thermal recuperator)
- **Radiant heat from rebars and wire rods**

## Summary

A synthesis of the collected data is presented in the schematic representation and summary table provided below, illustrating the main sources, energy media, and potential for recovery across the identified process areas.

The criteria applied to select the energy sources relevant to the project scope were agreed upon with the research partners as follows:

- Significance of the available thermal power
- Relevance of temperature flow that should enable a subsequent reuse for recovery (as for example temperatures > 300 °C)

The data presented are average values of continuously monitored parameters, as detailed below:

- EAF primary off-gas duct — upstream of the quenching tower
  - Off-gas flow rate measured by a Venturi detection system installed downstream of the quenching tower
  - Off-gas temperature continuously monitored upstream and downstream of the quenching tower by thermocouples
- EAF secondary off-gas duct (drawing from the internal steelshop atmosphere):
  - Off-gas flow rate derived from measurements taken at the single shared chimney, excluding the EAF primary cooling duct.
  - Off-gas temperature derived from global measurements, excluding the contribution of the primary duct.
- District heating water circuit:
  - Water flow rate measured by flow meters

- Temperature measured by thermocouples
- Reheating furnace off-gas duct:
  - Off-gas flow rate measured by a Venturi detection system installed downstream of the recuperator
  - Off-gas temperature continuously monitored upstream and downstream of the recuperator by thermocouples
- Furthermore, with particular regard to billet reheating, ongoing studies are being conducted to better characterise the thermal behaviour of the process, improve temperature monitoring and estimation, and support CO<sub>2</sub>/NO<sub>x</sub> emissions reduction. In particular, an enhanced off-gas monitoring system is planned for deployment in the next phase of the project.

Figure 1 illustrates the overall production cycle, encompassing both the steelmaking and rolling areas, and highlights the main zones considered for energy recovery evaluation, including the EAF, ladle furnace (LF), continuous casting, ladle preheating, and the reheating furnace for billet rolling. In the following, the volume flow units are given in normalized cubic meters per hour Nmc/h.

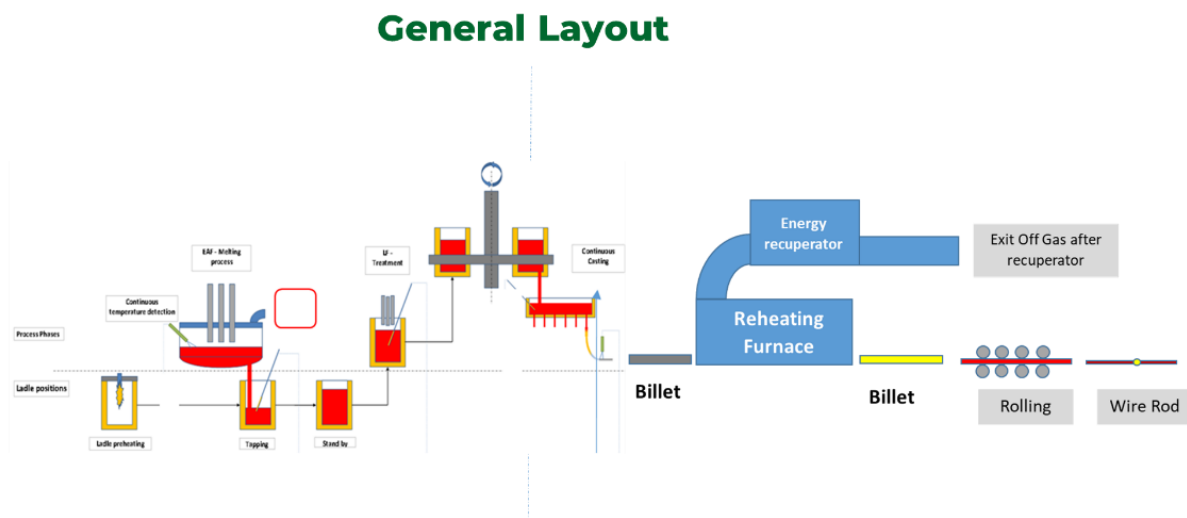


**Figure 1: General layout of the Feralpi Siderurgica plant illustrating the connection between the steelmaking (EAF, ladle, tundish) and rolling (reheating furnace, rolling mill) areas**

Figure 2 illustrates the main pathways of residual energy dispersion and the corresponding recovery potential, covering the EAF primary off-gas duct, the EAF secondary off-gas duct, and the district heating circuit.

Figure 3 provides a schematic view of the off-gas streams from ladle preheating. It should be noted that final measurement values are not yet available; this diagram therefore constitutes the basis for the further developments described in the subsequent phases of the project.

Figure 4 presents the configuration of the reheating furnace off-gas system, reporting flow rate and temperature values at the duct outlet, including the range of variability and the corresponding average values.

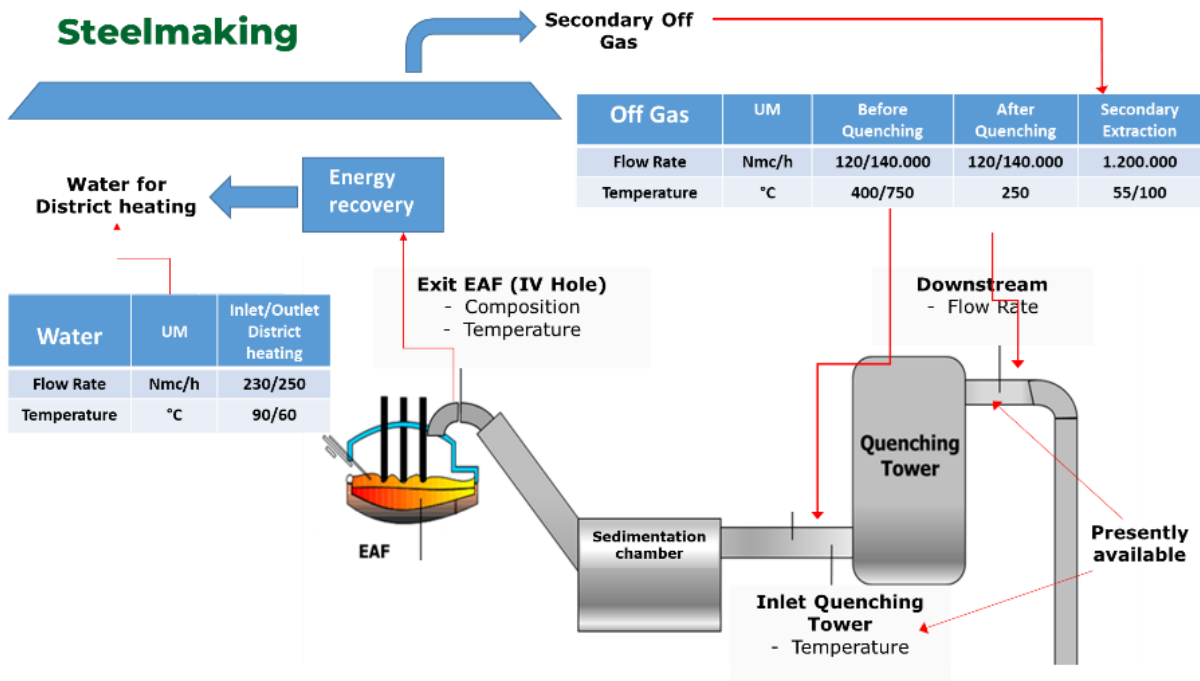


Figure 2: Schematic of the Steelmaking area focusing on EAF primary and secondary off-gas extraction and cooling water systems, including flow rates and temperature data

## Ladle Preheating

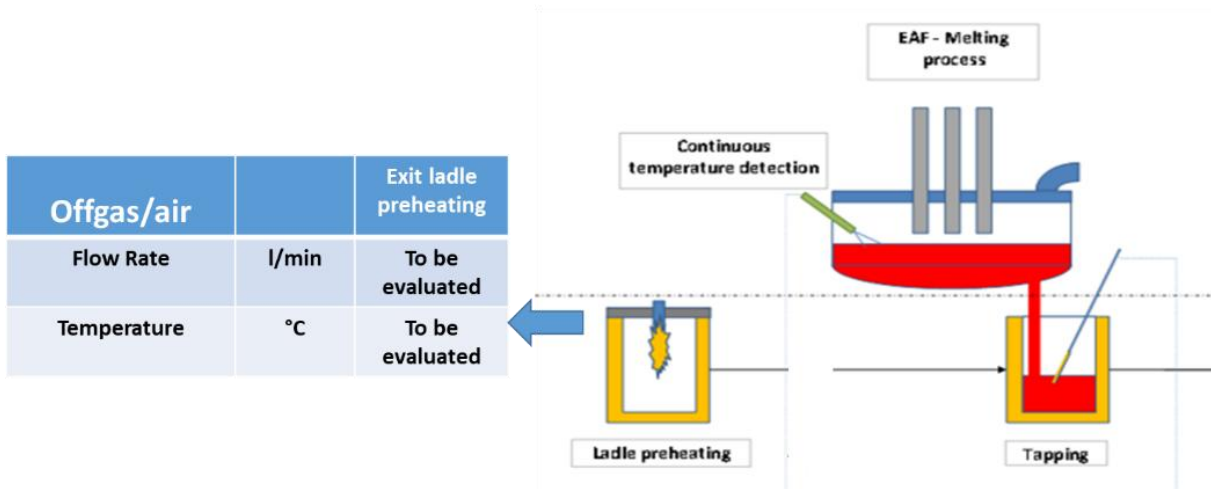


Figure 3: Representation of the Ladle Preheating and Tapping stations

## Rolling

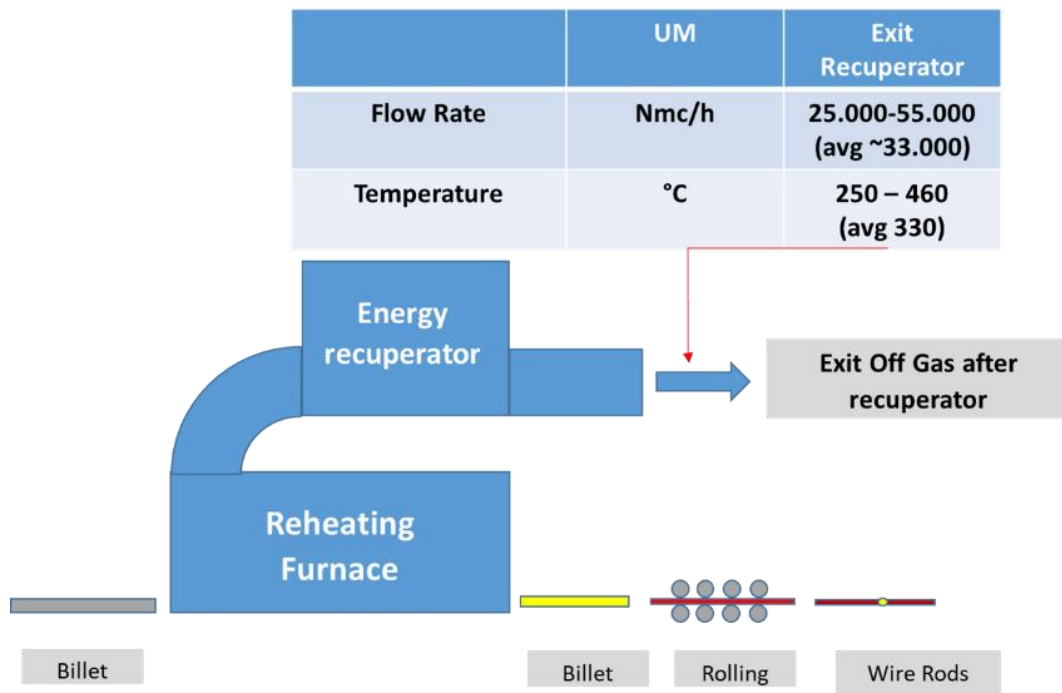


Figure 4: Schematic of the Rolling area focusing on the Reheating Furnace and Energy Recuperator, including off-gas temperature and flow rate data

## Summary data

Area	Section	Fluid	Temperature (°C)	Flow Rate (Nmc/h)
EAF	Off Gas – Before quenching	Off Gas	400/750	120/140.000
EAF	Off Gas – After quenching	Off Gas	250	120/140.000
EAF	Off Gas – Secondary	Off Gas	55-100	1.200.000
Acciaieria	Ladle Drying - preheating	Air	To be evaluated	
Acciaieria	Tundish Drying - preheating	Air	To be evaluated	
Laminatoio 2	Off gas billets preheating	Off Gas	250/460 (AVG 330)	25/55.000 (AVG 33.000)

**Figure 5: Summary table of the main heat sources identified at the Feralpi Siderurgica site, detailing fluid types, temperatures, and flow rates**

Figure 5 summarises the estimated values of the available dispersed energy across all identified sources.

### 2.2 Acciaierie d'Italia Site Analysis

It's well-known that the hot strip rolling process, consisting of heating the slabs in a furnace and rolling them in the stands, involves numerous heat losses. Some of these can be reduced (transferring of the bar through the roughing stands), while others are necessary to reach the target end-of-finishing rolling and coiling temperatures. As mentioned in the proposal of task 2.1, to pursue the evaluation of the heat losses reduction, it's important to quantify them considering the ADI case. For this reason, some scenarios were analyzed, and they are listed below.

1. Heat losses during the hot rolling, from the reheating furnace to the first finishing stand, considering a group of coils to represent a simplified rolling program
2. Heat losses of coils from the down coiler to the end of the stocking
3. Heat analysis of the skid beam cooling

#### Heat losses during hot rolling

To quantify the heat losses during hot rolling, for which it is possible to evaluate a possible recovery or reduction, 8 strips with different widths, thickness and qualities were considered to reproduce in a simplified way the rolling program (a group of strips with the same working rolls in the finishing stands). Since the steel grades considered had similar chemical compositions, the same thermal properties were used for all of

them. In addition, because different sizes of strips involve different strategies to roll them, the respective schedules were calculated considering similar last finishing stand temperatures, using an optimization algorithm based on differential evolution.

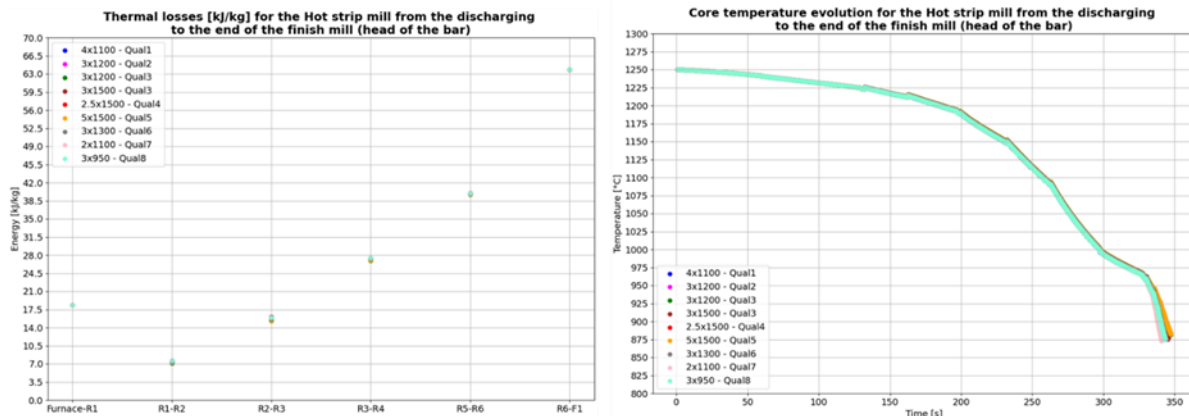


**Figure 6: Graph of the heat losses (left) and trend of the core temperature calculated (right) for the head of the bar**

All calculations were carried out considering the same length (9 m) and thickness of the slab (240 mm), using a thermo-mechanical model based on the Crank Nicolson approach, calibrated with temperatures and other parameters measured in the plant, to evaluate the thermal evolution of the bar subject to the radiation, convection, descaling, heat from deformation and conduction of the work rolls.

The Figure 6 shows the specific thermal losses calculated from the reheating furnace to the entry of the finishing mill and the respective trend of the core temperature calculated for the head of the bar. As expected, the highest thermal loss values are reached during the transferring of the bar after the sixth roughing stand (R6), due to the higher time and higher surface of the bar that increase the loss by radiation (about 64 kJ/kg). In addition, it's important to specify that higher loss of temperature in transferring of the bar to R1 (about 18 kJ/kg) respect to some passages is justified by the higher time where the slab is subject to heat loss by the sizing press and the descaling of the waterbox.

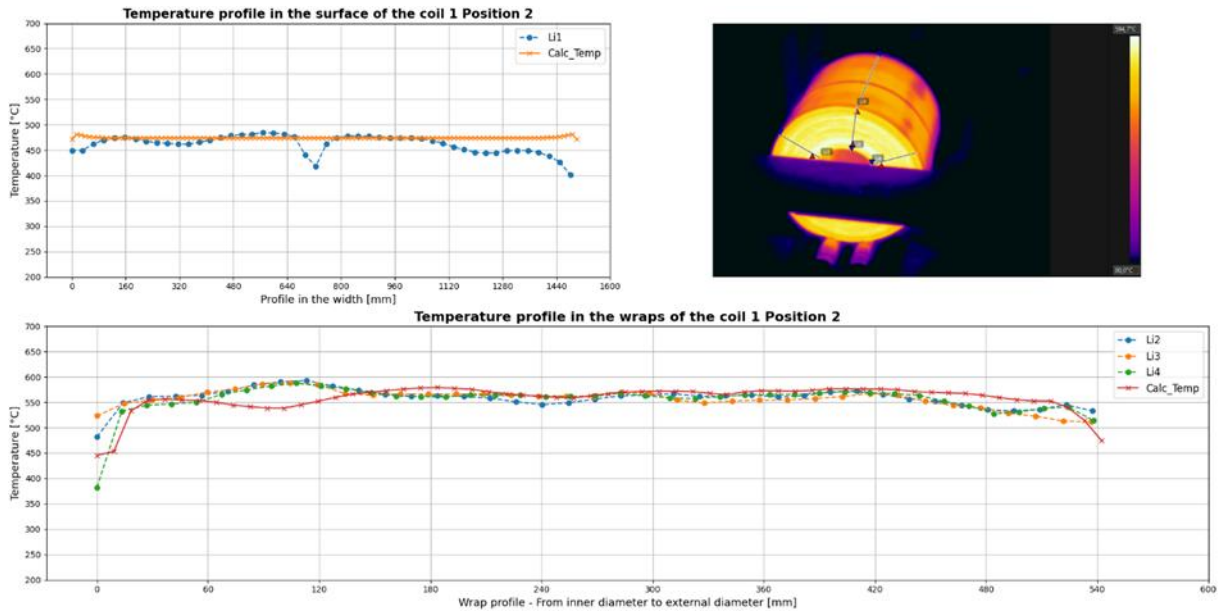


**Figure 7: Comparison between calculated and measured surface temperatures of one coil after its hot rolling**

### Heat losses of coils from the down coiler to the storage

In addition to the investigation of the hot rolling process, another interesting point of analysis is the heat loss of the coiled strip during its stocking in the warehouse before the shipment or the subsequent working. To quantify it, it was necessary to carry out measurements for 14 strips by a thermal camera to evaluate the surface temperature of the coils with different target coiling temperatures. All of these were conducted by positioning the camera at approximately 10 m from the coilers and setting an emissivity value of 0.8. All strips had a range of thickness between 2 mm and 2.8 mm, a width around 1500 mm, a mean coiling temperature between 550°C and 610 °C and an external coil diameter between 1850 mm and 2000 mm (Table 1).

Coil	External coil diameter [mm]	Thickness [mm]	Width [mm]	Average coiling temperature [°C]
1	1856	2.03	1513.1	610.5
2	1893	2.03	1510.7	608.0
3	1830	2.03	1509.5	609.0
4	1823	2.03	1510.7	609.3
5	1823	2.03	1509.5	603.9
6	1836	2.53	1537.3	580.2
7	1955	2.73	1518.3	550.9
8	1978	2.73	1512.7	554.4
9	1977	2.73	1513	550.4
10	1949	2.73	1511.1	554.6
11	1960	2.73	1513.9	550.8
12	2007	2.73	1514	556.5
13	1976	2.73	1512.5	551.5
14	1956	2.73	1512.5	550.8

**Table 1: Characteristics of the coils considered for the thermal measurements**

Since the device was unable to record video, three photos were taken in three different moments, for each coil considered:

- after the first coil strapping (Position 1)
- before the tilting of the coil into the transferring table (Position 2)
- after the tilting of the coil (Position 3)

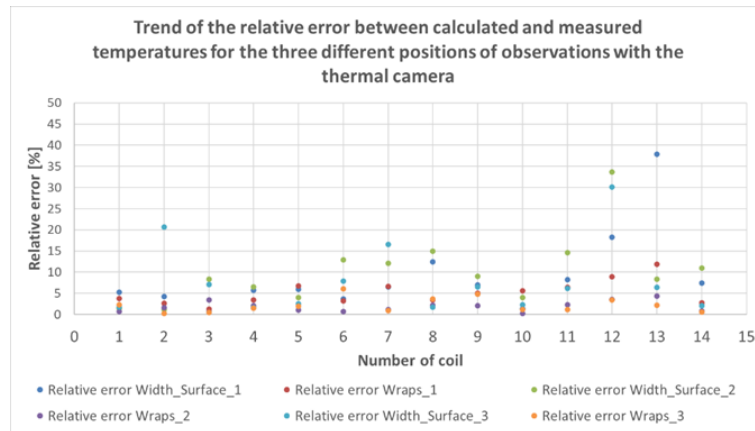


**Figure 8: Trend of the relative error for the different position between calculated and measured temperatures**

Following a similar approach to the hot rolling scenario, a thermal model was developed using the finite element method based on the Crank Nicolson approach (symmetry respect to the width of the coil and to the radius of the coil) and it was validated by a comparison with the temperature profiles extracted from the thermal camera maps, involving radiation and convection heat exchanges. As can be observed in Figure 7, the model was able to predict the temperature of the coil surface and the surface temperature of the wraps. In this regard, the Figure 8 shows the trend of relative error that is quite always less than 10%.

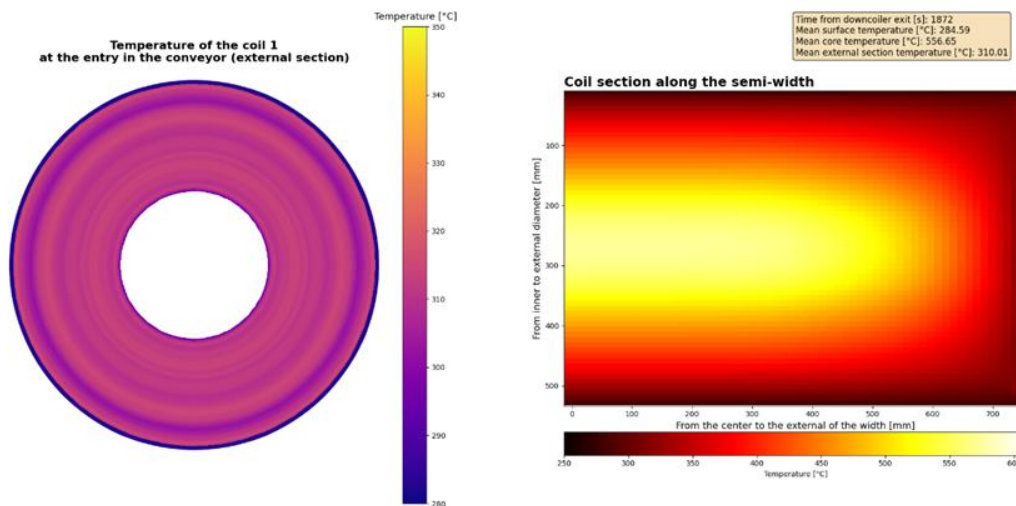


**Figure 9: Heat map of the coil 1 after the entry in the conveyor**

Having obtained a good correspondence between calculated and measured temperatures of the 14 coils, the temperature evolution was calculated in other different times (at the entry of the conveyor and at the end of the storage). An example of the heat maps is shown in the Figure 9 and the subsequent graph summarizes the temperature calculated for all coils after the end of storage; because the time from the

coiler to end of parking is similar, the mean temperature decreases after 75 minutes ranges from 380°C to 450°C (core section). This is confirmed by the observation of the graph (Figure 10) that resumes the mean temperatures calculated for all strips.

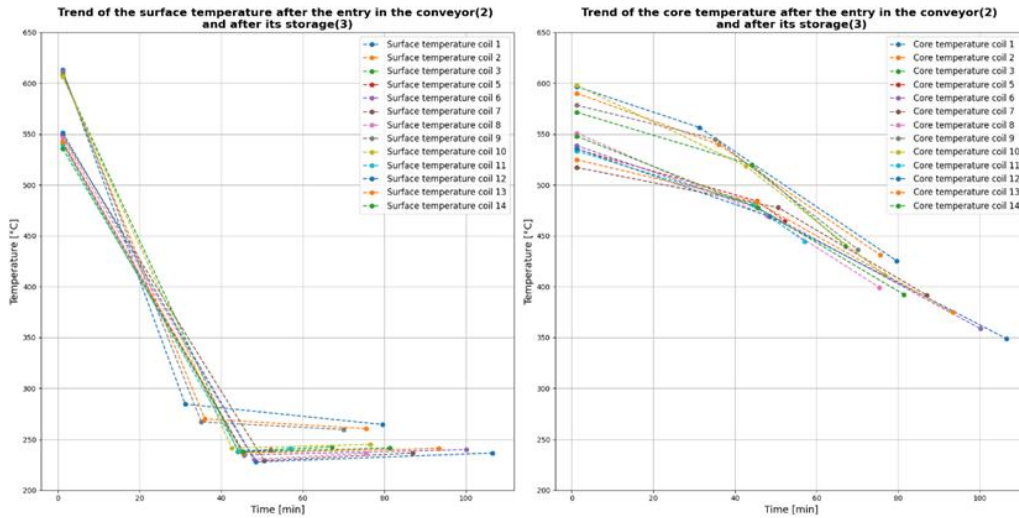


**Figure 10: Surface and core temperatures calculated after the entry into the conveyor for next strapping and after the stocking of the coils considered in the thermal measurements**

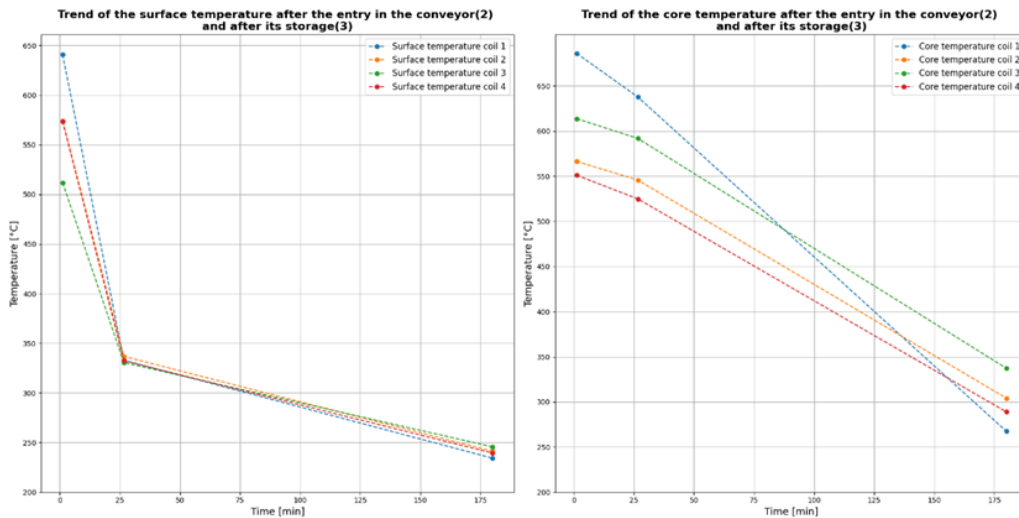


**Figure 11: Surface and core temperatures calculated after the entry into the conveyor for next strapping and after the stocking of the coils in the simulation**

Subsequently, a simulation of 4 coils (see Table 2) was carried out to calculate the evolution of the temperature after a half hour and three hours from the coiling. The coils have a thickness of around 2 mm, a range of width from 1000 mm to 1600 mm and a target coiling temperature that ranges from 550°C to 700°C. From this point of view, in the Figure 11 it's possible to see how the temperature of the coil (core) decreases of more than 250°C in the core coil section and the surface temperature reaches

values near to 230°C after 3 hours. These measurements are similar to the temperatures measured for a similar scenario<sup>1</sup>.

Coil	External coil diameter [mm]	Thickness [mm]	Width [mm]	Average coiling temperature [°C]
1	1634	2.24	1284.2	696
2	2016	2	1282.3	559
3	2101	2.76	1517	610
4	1985	2.1	1018	550

**Table 2: Characteristics of the coils considered for the simulation**

### Heat loss from the skid beam cooling

Typically, the cooling of the skids represents the 10÷15% of furnace heat losses. This percentage is confirmed also considering the specific case of ADI with its five furnaces of the hot strip mill 2. In this regard, the skid beam cooling between furnaces is different: in the first three furnaces (1, 2, and 3) we have a flow rate (for each furnace) of about 2500 m<sup>3</sup>/h and a  $\Delta T$  (difference between entry and exit temperatures) of about 5 °C, and for the last furnaces the flow rate is about 500 m<sup>3</sup>/h with a  $\Delta T$  of about 20°C. To confirm it, some collected data were considered, recording the flow rate and the temperatures of the skids in some days for the furnace 1.

However, as can be observed in the figure,  $\Delta T$  ranges from 3.8°C to 5 °C and based on it, the related lost energy ranges from 9600 Mcal/h to 13000 Mcal/h.

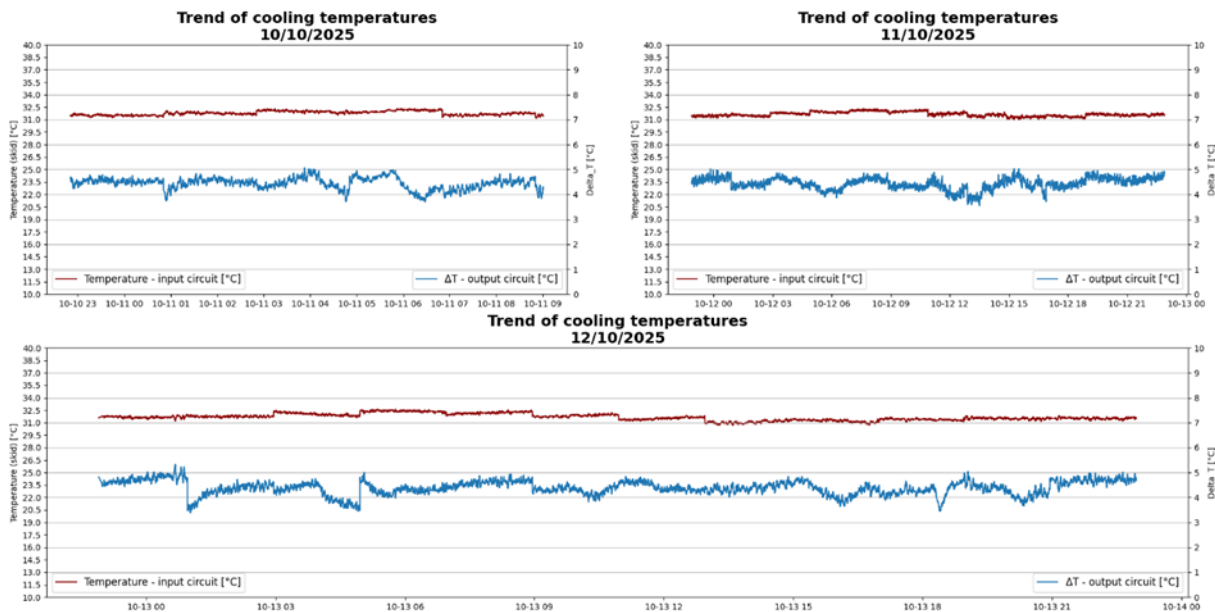


**Figure 12: Trend of the overall difference between exit and entry temperatures for the furnace 1**

<sup>1</sup> Yousaf, N. (2009). Calculation of waste heat from hot rolled steel coils at SSAB and its recovery (Dissertation). Retrieved from <https://urn.kb.se/resolve?urn=urn:nbn:se:du-4516>

### 3. Theoretical Framework for Heat Recovery

#### 3.1 Thermodynamic principles for waste heat recovery

Waste heat recovery in steelmaking downstream processes is governed by fundamental thermodynamic principles that dictate the feasibility and efficiency of energy recovery systems<sup>2</sup>. The first law of thermodynamics establishes that energy cannot be created or destroyed, only transformed from one form to another; thus, the thermal energy released in off-gases, cooling water, or as radiant heat in steelmaking operations constitutes a source of recoverable heat flow with defined thermal power content. The second law of thermodynamics, however, implies that the quality of thermal energy—i.e., its capacity to perform useful work—decreases with temperature reduction. This thermodynamic quality is quantified through exergy analysis, which evaluates the maximum theoretical work extractable from a thermal stream relative to the environment. Therefore, exergy analysis is very useful to evaluate thermal transfer efficiency and process irreversibility.

In the context of the first stages of E-ECO Downstream project, waste heat recovery is evaluated using mass and energy balance equations that account for the thermal characteristics of identified heat sources. At this stage, some simplifications have been introduced.

The recoverable heat flow rate  $\dot{Q}$ , is fundamentally determined by the product of the mass flow rate of the hot stream ( $\dot{m}$ ), its specific heat capacity ( $c_p$ ), and the temperature difference available for heat exchange ( $\Delta T$ ):

$$\dot{Q} = \dot{m}c_p(T - T_0)$$

On the other hand, the exergy flow rate (maximum useful work rate extractable from the hot stream relative to the environment, neglecting chemical exergy) is computed for a constant- $c_p$  gas as:

$$\dot{Ex} = \dot{m}c_p \left[ (T - T_0) - T_{env} \ln \left( \frac{T}{T_0} \right) \right]$$

with temperatures in Kelvin. Then,  $T_{env}$  is set to 298K.

The choice of  $T_0$  is critical for realistic heat recovery estimates and depends on the specific application and operational constraints:

- For high-temperature off-gases ( $> 400^\circ\text{C}$ ) with recuperation before existing quenching systems:  $T_0 = 200^\circ\text{C}$  is used as the post-recovery discharge temperature. This reflects practical limitations where gases entering the

---

<sup>2</sup> European Commission, “Best Available Techniques Reference Document (BREF) – Iron, Steel and Non-Ferrous Metals Production,” 2013. Available: <https://publications.jrc.ec.europa.eu/repository/handle/JRC69967>

quenching tower must remain sufficiently hot to maintain tower effectiveness and prevent acid sludge formation. The quenching tower can then operate at a reduced regime (if recovery achieves 200-250°C) or at full capacity (if no recovery is implemented), providing operational flexibility. Moreover, this temperature allows avoiding issues in fabric filters in gas treatment systems.

- For medium-temperature off-gases (250-400°C):  $T_0 = 80^\circ\text{C}$  represents the minimum atmospheric discharge temperature required to prevent acid condensation, protect fabric filters in gas treatment systems and ensure proper gas suction in the chimney for pollutant dispersion.
- For low-temperature sources already near ambient ( $< 250^\circ\text{C}$ ):  $T_0 = 25^\circ\text{C}$  can be appropriate as these streams can be cooled closer to ambient without operational issues.
- $T_0 = 25^\circ\text{C}$  is also used in all the evaluated case as reference value for computing the **theoretical** maximum recoverable heat.

Unless otherwise specified, all numerical evaluations in this deliverable, involving gas streams, use  $c_p = 1.2 \text{ kJ}/(\text{kg}\cdot\text{K})$  (i.e. a good assumptions for high temperature, and  $\text{CO}_2$  and  $\text{H}_2\text{O}$  containing gas, that have a higher  $c_p$  than dry air having a  $c_p = 1.0 \text{ kJ}/(\text{kg}\cdot\text{K})$ ). This represents a simplified constant-property model; refined engineering design should account for temperature-dependent thermophysical properties and actual off-gas composition. EAF off-gas and reheating furnaces off gases, containing mainly  $\text{CO}$ ,  $\text{CO}_2$ ,  $\text{N}_2$ ,  $\text{H}_2\text{O}$ , and  $\text{O}_2$  (in case of air/ $\text{O}_2$  excess) exhibits  $c_p$  in the range 0.9–1.4  $\text{kJ}/(\text{kg}\cdot\text{K})$  and 1.1-1.3  $\text{kJ}/(\text{kg}\cdot\text{K})$ , respectively; detailed calculations should include composition-specific properties. However, their ranges show that the assumption is correct.

As an example, for the Electric Arc Furnace (EAF) *primary* off-gas stream characterized in the FER site thermal mapping (average 130,000  $\text{Nm}^3/\text{h} \approx 46.6 \text{ kg/s}$  using a density of 1.29  $\text{kg}/\text{Nm}^3$ ), the sensible heat flow rate and exergy flow rate are evaluated at different source temperatures and discharge conditions.

With  $T_0 = 200^\circ\text{C}$ :

- $T = 400^\circ\text{C} \rightarrow$  sensible heat flow rate  $\approx$  **11.2 MW**, exergy flow rate  $\approx$  **5.3 MW**
- $T = 575^\circ\text{C}$  (average)  $\rightarrow$  sensible heat flow rate  $\approx$  **21.0 MW**, exergy flow rate  $\approx$  **11.2 MW**
- $T = 750^\circ\text{C} \rightarrow$  sensible heat flow rate  $\approx$  **30.8 MW**, exergy flow rate  $\approx$  **17.9 MW**

With  $T_0 = 25^\circ\text{C}$  (theoretical maximum, for reference only):

- $T = 400^\circ\text{C} \rightarrow$  sensible heat flow rate  $\approx$  **21.0 MW**, exergy flow rate  $\approx$  **7.4 MW**
- $T = 575^\circ\text{C}$  (average)  $\rightarrow$  sensible heat flow rate  $\approx$  **30.8 MW**, exergy flow rate  $\approx$  **13.3 MW**
- $T = 750^\circ\text{C} \rightarrow$  sensible heat flow rate  $\approx$  **40.5 MW**, exergy flow rate  $\approx$  **20.0 MW**

These values demonstrate key points: (1) exergy is considerably smaller than sensible heat and increases non-linearly with temperature; (2) realistic discharge temperatures significantly reduce recoverable energy compared to theoretical calculations—for the 575°C case, recoverable power drops from 30.8 MW (theoretical) to 21 MW ( $T_0 = 200^\circ\text{C}$ ), representing a >30% reduction; (3) exergy must be used when assessing suitability for power generation applications but is also extremely useful for thermal transfer applications analyses. The calculations above neglect chemical exergy (no fuel-rich or reactive chemical exergy is included here). Full thermodynamic potential assessment would include these terms via standard chemical exergy formulations<sup>3</sup>. However, for preliminary source ranking, sensible exergy dominates the total available exergy.

Sensible heat can be used to heat up another flow (e.g., combustion air or fuel) through a heat exchanger. Typical heat exchanger efficiencies for industrial recuperators range from 60% to 80% depending on design (plate exchangers, regenerative systems, or tubular recuperators). Regenerative exchangers achieve 85–90% thermal efficiency under steady-state cyclic operation. Pinch-point constraints must be applied in practical heat exchanger design. When designing a recuperator for air preheating, a  $\Delta T_{min}$  consistent with the heat-exchanger technology and fouling/pressure-drop trade-offs (typical values: 20–40°C) should be chosen. The minimum approach affects the cold-side target temperature and the achievable outlet temperature of the hot stream; the design procedure therefore must iterate between required preheat temperature,  $\Delta T_{min}$  and the available hot-stream temperature to compute the actual recoverable heat and associated exergy.

For off-gases from the Electric Arc Furnace (EAF) primary duct and reheating furnace exhaust, temperature levels typically range from 400 to 800°C downstream of already existing quenching towers or recuperators, presenting significant sensible heat and exergy content still available. Conversely, lower-temperature streams from EAF cooling systems (typically 40–80°C) and auxiliary cooling circuits offer energy with lower thermodynamic quality but may serve niche applications such as district heating or process water preheating with appropriate integration.

When designing recuperators or regenerators for preheating oxidizers or fuels with exhaust gases from hydrogen-enriched or pure hydrogen combustion, the specific properties of these future fuels must be considered. Hydrogen exhibits a significantly higher flame temperature (approximately 2,180–2,250°C in air) compared to natural gas (approximately 1,900–1,960°C), altered combustion kinetics, and different exhaust gas composition—particularly reduced CO<sub>2</sub> and increased H<sub>2</sub>O content. These variations necessitate thermodynamic recalculation of available exergy for heat recovery devices. Additionally, when considering biofuels as transition fuels, their

---

<sup>3</sup> M. J. Moran, H. N. Shapiro, D. D. Boettner, and M. B. Bailey, *Fundamentals of Engineering Thermodynamics*, 9th ed. Hoboken, NJ: Wiley, 2018

proximate and ultimate analyses affect stoichiometric combustion calculations and energy balances.

The thermodynamic assessment therefore focuses on calculating the net energy balance—accounting for the losses of heat recovery equipment operation against the recovered thermal energy—to determine true net efficiency gains and economic viability under realistic industrial conditions.

### Implications for Source Selection

The disparity between sensible heat and exergy dictates the allocation strategy. High-exergy sources possess high thermodynamic quality, meaning they can drive high-temperature processes (such as preheating combustion air to 400°C) or generate electricity. Utilizing high-exergy streams for low-grade applications (e.g., heating water to 60°C) results in significant exergy destruction—essentially wasting the “work potential” of the energy. Therefore, a cascaded recovery strategy is required: low-exergy streams must be relegated to low-temperature sinks like district heating, regardless of their total thermal mass.

## 3.2 Heat recovery technologies overview

Possibilities for heat recovery comprise recuperators, regenerators, central heat recovery units and self-recuperative burners.

Recuperators work continuously and allow for reduction in fuel consumption up to 30% when compared to processes without heat recovery. Central heat recovery units enable large amount of energy but are limited to 500-600 °C in preheating.

Regenerators work discontinuously while allowing highest preheating temperatures up to 1100°C. They come with higher investment costs for the increased amount of instruments and equipment. Most available systems operate with local systems plugged directly to the burner. In comparison to central recuperators, the reduction in fuel consumption lies between 10% in continuous processes and up to 30% for batch furnaces when applying regenerators.

Burners with integrated heat recovery by recuperator (self-recuperative burner) or regenerator are limited in output and have the tendency to clog. In industry they are in operation in heat treatment furnaces.

On the plant site of Feralpi the concept of heat recovery by central recuperators with respect to the combustion air is already successfully under use.

Aside from this existing application we suggest the further consideration of heat recovery techniques with respect to fuel preheating. As the ratio of fuel to combustion air increases towards the fuel portion with the growing amount of hydrogen within the mixture, the effect of preheating becomes increasingly more effective. To date, this option was not considered as the ratio of natural gas and combustion air was approximately 1:10, and hence the impact was almost negligible.

In case of local requirements towards warm water provision on site, the use of heat pumps is considered. Using heat pumps within an industrial context is of minor interest, since the attainable temperature is too low. But the warm water supply for some of the on-site facilities can be provided, even though the resulting recovered heat is negligible when accounting the industrial demand at Feralpi.

### 3.3 Preheating strategies

Preheating strategies represent a primary mechanism for utilizing recovered waste heat to enhance the energy efficiency of reheating furnaces in downstream steelmaking processes. The fundamental principle underlying preheating is the reduction of energy demand in the main furnace by elevating the inlet temperature of process streams—whether fuel, oxidizer (air or oxygen-enriched air), or their combinations—prior to combustion or heating. This approach has well-established theoretical benefits: for a given final product temperature and furnace efficiency, reducing the temperature lift required within the furnace reduces fuel consumption proportionally<sup>4</sup>.

#### Fuel preheating

Fuel preheating involves heating the gaseous or liquid fuel stream using available waste heat prior to combustion. In the context of future fuels investigated within the E-ECO Downstream project, fuel preheating strategies must account for distinct characteristics of hydrogen, biofuels, and fuel blends. For hydrogen, whether used as a pure fuel or in natural gas–hydrogen blends, moderate preheating of the reactants (on the order of 100–150°C) increases the mixture enthalpy and reaction rates, which raises the flame temperature and combustion intensity; in a furnace this can enhance local heat transfer, although the overall efficiency gain depends on the specific system design and operating conditions. However, hydrogen's inherently higher flame temperature and rapid combustion kinetics necessitate careful consideration of burner aerodynamics and furnace material compatibility to prevent localized overheating. Biofuels, conversely, may exhibit greater preheating tolerance due to their similar composition to conventional hydrocarbon fuels, though their variable moisture content and potential for polymerization at elevated temperatures impose practical constraints. The pilot-scale experimental investigations will validate fuel preheating performance with actual retrofitted burners, providing empirical data on combustion stability, NO<sub>x</sub> emissions, and heat transfer characteristics under conditions representative of industrial reheating furnaces.

#### Oxidizer (air/oxygen-enriched) preheating

Oxidizer (air/oxygen-enriched) preheating constitutes an alternative or complementary preheating strategy wherein the combustion air (or oxygen-enriched air) is preheated using exhaust gases from the furnace via a recuperator. This approach is particularly

---

<sup>4</sup> J. M. Smith, H. C. Van Ness, and M. M. Abbott, Introduction to Chemical Engineering Thermodynamics, 7th ed. New York: McGraw-Hill, 2005.

effective in reheating furnaces because preheating the combustion air raises the flame and bulk gas temperatures, which increases radiative heat transfer and, through the larger gas–steel temperature difference and modified flow properties, enhances the overall gas-side heat transfer to the stock. Conventional air preheating to temperatures of 200–400°C is well-established in industrial practice.

### Mixed strategies

Mixed strategies (simultaneous fuel and oxidizer preheating or cascaded multi-stage heat recovery) typically yield the largest site-level energy savings. All mixed designs must explicitly model exergy flows (not only sensible heat) to avoid suboptimal allocation of high-quality heat to low-value uses.

## 3.4 Compatibility with future fuels (H<sub>2</sub>, biofuels)

The transition toward decarbonized steel production necessitates fundamental reassessment of waste heat recovery system design to ensure compatibility with future fuel compositions and combustion characteristics. Hydrogen (H<sub>2</sub>) and biofuels represent the primary candidates for replacing fossil natural gas in downstream steelmaking reheating processes within the E-ECO Downstream project's scope, yet their distinct thermochemical properties introduce both opportunities and constraints for heat recovery system performance.

### Hydrogen Combustion Characteristics

Hydrogen combustion presents unique thermodynamic and chemical characteristics that necessitate adapted heat recovery designs. The complete combustion of hydrogen in air produces significantly higher flame temperatures (approximately 2,180–2,250°C) compared to approximately 1,900°C for natural gas stoichiometric combustion<sup>5</sup>, implying enhanced local radiative intensity to furnace loads. However, this thermodynamic advantage is partially offset by distinct radiative characteristics: hydrogen flames exhibit lower radiative emissivity and minimal soot formation compared to methane flames, resulting in a net radiative heat flux increase of approximately 15–25% despite their higher adiabatic temperatures.

The higher hydrogen flame temperature leads also to the increase of off-gas temperature, that, although can improve the thermal efficiency, can improve the thermal NO<sub>x</sub> formation; however new hydrogen burners are designed to avoid this issue.

More critically, hydrogen combustion generates substantially higher water vapor concentrations—approximately 9 kg H<sub>2</sub>O per kilogram of H<sub>2</sub> combusted, compared to approximately 2.2–2.5 kg H<sub>2</sub>O per kilogram of natural gas—fundamentally altering exhaust thermophysical properties and elevating dew point temperatures to 80–100°C (at process pressures) compared to 50–60°C for natural gas systems. This

---

<sup>5</sup> S. R. Turns, *An Introduction to Combustion: Concepts and Applications*, 3rd ed. New York: McGraw-Hill, 2012.

composition shift from stoichiometric natural gas combustion (approximately 20–25 vol.% H<sub>2</sub>O, 8–10 vol.% CO<sub>2</sub> in case of combustion with air) to hydrogen combustion (approximately 30–35 vol.% H<sub>2</sub>O, <0.1vol.% CO<sub>2</sub> in case of combustion with air) substantially modifies the thermal properties of off-gases, including specific heat capacity and radiative emissivity, requiring fundamental recalculation of heat exchanger designs previously optimized for natural gas operation.

Moreover, for the same amount of thermal energy produced and assuming stoichiometric combustion conditions, the use of hydrogen implies a mass reduction of off-gases.

Additionally, hydrogen exhibits a considerably wider flammability range in air (4–75%) compared to natural gas (5–15%), though the optimal combustion window for stable burner operation is narrower, constraining operational flexibility during transient conditions and demanding burner redesign to prevent flame extinction or instability.

### **Material Compatibility for Hydrogen Combustion**

Recuperators and regenerators must be rigorously evaluated for material compatibility under the altered exhaust gas composition and enhanced thermal stresses imposed by hydrogen combustion. The candidate materials identified for recuperator construction—including advanced Ni-base superalloys capable of long-term exposure to 1,200°C in air—must demonstrate robust resistance to hydrogen-induced stress corrosion cracking (HISCC) and hydrogen embrittlement (HE), failure modes particularly acute in high-strength, high-temperature nickel alloys exposed to hydrogen-rich combustion atmospheres.

Research demonstrates that Ni-base superalloys exhibit temperature-dependent hydrogen susceptibility, with maximum embrittlement typically occurring in the 200–700°C range rather than at the highest service temperatures. At very high temperatures (>1000°C), thermodynamic factors substantially reduce HE severity; however, sustained tensile stresses during thermal cycling or transient operations can initiate HISCC. Material selection must therefore balance intrinsic alloy strength, design stress levels, operational temperature profile and pilot-scale validation.

### **Biofuel compatibility**

Biofuel compatibility considerations differ substantially from hydrogen, as biofuels (including sustainable aviation fuel derivatives and biogas-derived energy carriers) maintain chemical composition and combustion characteristics more closely aligned to conventional hydrocarbon fuels, particularly regarding adiabatic flame temperature and bulk exhaust gas composition. However, biofuels introduce distinct challenges related to ash formation and deposition, enhanced corrosion potential, and thermal polymerization of oxygenated organic compounds.

Heat recovery system design adaptation to future fuels must systematically address corrosion kinetics, material degradation mechanisms, and optimal operating temperature profiles.

## 4. Selection and Prioritization of Heat Sources

### 4.1 Selection Methodology

Heat-source prioritization follows four steps:

1. **Thermal characterization:**  
Record temperature, flow and composition.
2. **Energy/exergy evaluation:**  
Compute sensible heat flow rate:

$$\dot{Q} = \dot{m}c_p(T - T_0)$$

and exergy:

$$\dot{E}x = \dot{m}c_p[(T - T_0) - T_{env}\ln(T/T_0)]$$

3. **Technical feasibility:**  
Assess duct routing, fouling tendency, corrosion, abrasion, particulate load, pressure drop, and maintenance access. Sources requiring excessive plant modifications or presenting operational risks are deferred to medium-term scenarios unless energy recovery potential is exceptionally high.
4. **Fuel-transition compatibility:**  
Consider implications for new fuels combustion with particular focus on hydrogen since biofuels types and features are multiple and a more detailed analysis is required: increased water vapor content, elevated flame temperature, and corrosion risks in heat exchanger materials.

Streams with high exergy density are prioritized for air/fuel preheating for use within the process; low-temperature, high-mass-flow streams are directed to district heating or water-preheating applications for use outside the process.

### 4.2 Feralpi Siderurgica Priority Sources

Application of the selection methodology outlined in Section 4.1 to the thermal mapping data collected at the FER site yields a prioritized hierarchy of waste heat sources suitable for preheating strategies. The analysis focuses exclusively on sources applicable to preheating applications in reheating furnaces and related heating processes, balancing exergy content, operational continuity, and retrofit complexity.

Possibilities for heat recovery from exhaust gas as described in chapter 3.2, where analyzed for applying suitable technologies at the production plant of Feralpi.

On the plant site of Feralpi the concept of heat recovery with respect to the combustion air is already successfully under use. Further increase of air temperature would require the replacement of piping, fittings and burners. Appropriate equipment for operation at

temperatures above 500 °C is significantly more expensive due to an increased insulation.

Aside from this existing application SSSA suggests the further consideration of heat recovery techniques with respect to fuel preheating. As the ratio of fuel to combustion air increases towards the fuel portion with the growing amount of hydrogen within the mixture, the effect of preheating becomes increasingly more effective. To date this option was not considered as the molar ratio of natural gas and combustion air was approximately 1:10, and hence the impact negligible.

The evaluation of the recoverable waste energy was carried out assuming a fixed off-gas composition. In reality, however, the off-gas composition can vary significantly, which affects the available energy. In some cases, the actual energy may be up to 30% lower than the estimated value. Therefore, the estimated values should be considered a project reference, while real operating conditions may result in lower energy availability depending on the actual off-gas composition.

While heat pumps offer a path toward electrification, their application at the Feralpi production plant remains secondary due to the high-grade thermal requirements of steel manufacturing. Currently, industrial-scale heat pumps are of minor interest for core processes because the attainable temperatures are significantly lower than those required for steel smelting and processing.

However, the local context of Lonato presents a specific opportunity for low-grade heat recovery. The waste heat generated from the active cooling of furnace equipment—specifically the hearth and transporting systems—can be repurposed for district heating or providing a warm water supply for onsite facilities. While the volume of heat recovered for these purposes is negligible compared to Feralpi’s total industrial energy demand, it serves as a critical link in integrating the plant with the Lonato community’s heating infrastructure.

## Priority 1: EAF Off-Gas Before Quenching

### *Thermal characterization*

**Flow:** average 130,000 Nm<sup>3</sup>/h → **46.6 kg/s**

**Temperature:** 400–750°C (average 575°C)

### *Energy/exergy evaluation*

Given the high source temperatures and the configuration with recovery before the existing quenching tower, a realistic discharge temperature of  $T_0 = 200^\circ\text{C}$  is used to reflect practical operational constraints.

Sensible heat flow rate and exergy flow rate with  $T_0 = 200^\circ\text{C}$ :

- 400°C → **11.2 MW** (sensible heat), **5.3 MW** (exergy)
- 575°C (average) → **21.0 MW** (sensible heat), **11.2 MW** (exergy)

- 750°C → **30.8 MW** (sensible heat), **17.9 MW** (exergy)

For reference, theoretical maximum with  $T_0 = 25^\circ\text{C}$ :

- 400°C → **21.0 MW** (sensible heat), **7.4 MW** (exergy)
- 575°C (average) → **30.8 MW** (sensible heat), **13.3 MW** (exergy)
- 750°C → **40.5 MW** (sensible heat), **20.0 MW** (exergy)

The EAF off-gas upstream of the quenching system emerges as the highest-priority heat source for preheating strategies at FER based on both thermodynamic and practical considerations. This stream exhibits exceptional thermodynamic quality: the high temperature permits substantial temperature lifts for both oxidizer and fuel preheating without violating pinch point constraints. For example, preheating combustion air from ambient temperature ( $25^\circ\text{C}$ ) to  $350^\circ\text{C}$  requires approximately 328 kJ/kg of air. Given the available off-gas temperature of  $575^\circ\text{C}$  (average) and a realistic discharge temperature of  $200^\circ\text{C}$ , typical heat exchanger efficiency of 70–75%, substantial air preheating is achievable. The high sensible heat content also enables fuel preheating to  $100$ – $150^\circ\text{C}$ , which enhances combustion intensity and flame temperature, particularly relevant when transitioning to hydrogen or hydrogen-natural gas blends.

The post-recovery discharge temperature of  $200^\circ\text{C}$  allows the existing quenching tower to operate at reduced regime (providing operational flexibility) or at full capacity if heat recovery is not implemented. This temperature is sufficiently high to maintain quenching tower effectiveness and prevent acid sludge formation.

Preheated air can be utilized in heat treatment furnaces as well as for preheating steel before it is charged into reheating furnaces. For the Feralpi layout, the most suitable application appears to be the current one: using preheated air to improve the efficiency of the existing heat treatment furnace, with the possibility of further optimization. Using preheated air for a preliminary steel preheating phase requires a more detailed technical and economic feasibility analysis. Specifically, the high investment costs—driven by limited space for a preheating station—may outweigh the potential benefits, making the project cost-ineffective.

### **Technical feasibility**

EAF off-gas ductwork at FER provides potential integration points for recuperator installation upstream of the existing quenching system. The off-gas composition—predominantly  $\text{N}_2$ ,  $\text{CO}$ ,  $\text{CO}_2$ ,  $\text{H}_2\text{O}$ , and particulate matter—necessitates dust removal or filtration upstream of heat exchangers to prevent fouling and erosion of recuperator surfaces.

### **Future fuel compatibility**

When FER's EAF burners transition to hydrogen or hydrogen-enriched fuel blends, the off-gas mass amount, temperature and composition will evolve. Considering that the

highest amount of EAF off-gases is generated from metallurgical reactions, the foreseen mass reduction due to Hydrogen combustion in EAF burners is limited from the point of view of the whole EAF off-gases. For the same amount of energy generated through hydrogen burners, a decrease lower than 7% is reasonable as first estimate. Hydrogen combustion generates exhaust gases with elevated H<sub>2</sub>O content and potentially higher exhaust temperatures due to hydrogen's elevated flame temperature; it can be assumed less than 3% but obviously it depends from several process and design aspects. Specific heat capacity is expected to increase; it can be assumed less than 4%.

Although these changes tend to compensate each other, they will affect the thermal power, which can increase or decrease depending on the predominant variation, and corrosion potential of the off-gas stream.

For the sake of clarity, sensible heat flow rate and exergy have been recalculated with the following assumptions:

- Mass reduction of 5% → **44.3 kg/s**
- Temperature increase of 2% → **408°C, 587°C, 765°C**
- Specific heat capacity increase of 3% → **1.24 kJ/(kg·K)**

With  $T_0 = 200^\circ\text{C}$ :

- $408^\circ\text{C} \rightarrow$  **11.4 MW** (sensible heat), **5.5 MW** (exergy)
- $587^\circ\text{C} \rightarrow$  **21.2 MW** (sensible heat), **11.5 MW** (exergy)
- $765^\circ\text{C} \rightarrow$  **31.1 MW** (sensible heat), **18.2 MW** (exergy)

For reference, with  $T_0 = 25^\circ\text{C}$  (theoretical):

- $408^\circ\text{C} \rightarrow$  **21.0 MW** (sensible heat), **7.5 MW** (exergy)
- $587^\circ\text{C} \rightarrow$  **30.9 MW** (sensible heat), **13.5 MW** (exergy)
- $765^\circ\text{C} \rightarrow$  **40.6 MW** (sensible heat), **20.2 MW** (exergy)

It can be observed that changes in the assumed conditions are almost negligible.

The selection of advanced materials (Ni-base alloys with demonstrated resistance to hydrogen-induced stress corrosion cracking and high-temperature oxidation) ensures that recuperators installed for this priority source will maintain performance and reliability under future operating conditions.

## Priority 2: Roll Mill 2 Off-Gas from Billet Preheating

### *Thermal characterization*

**Flow:**  $\approx 33,000 \text{ Nm}^3/\text{h} \rightarrow 11.8 \text{ kg/s}$

**Temperature:** 250–460°C (average 330°C)

### **Energy/exergy evaluation**

For this medium-temperature source discharging to atmosphere, a realistic discharge temperature of  $T_0 = 80^\circ\text{C}$  is used to prevent acid condensation and ensure proper atmospheric dispersion.

Sensible heat flow rate and exergy flow rate with  $T_0 = 80^\circ\text{C}$ :

- $250^\circ\text{C} \rightarrow$  **2.4 MW** (sensible heat), **0.8 MW** (exergy)
- $330^\circ\text{C}$  (average)  $\rightarrow$  **3.5 MW** (sensible heat), **1.3 MW** (exergy)
- $460^\circ\text{C} \rightarrow$  **5.4 MW** (sensible heat), **2.3 MW** (exergy)

For reference, theoretical maximum with  $T_0 = 25^\circ\text{C}$ :

- $250^\circ\text{C} \rightarrow$  **3.2 MW** (sensible heat), **0.8 MW** (exergy)
- $330^\circ\text{C}$  (average)  $\rightarrow$  **4.3 MW** (sensible heat), **1.3 MW** (exergy)
- $460^\circ\text{C} \rightarrow$  **6.2 MW** (sensible heat), **2.4 MW** (exergy)

The off-gas exhaust from the billet preheating furnace in Roll Mill 2 constitutes the second-priority heat source for preheating strategies at FER. The moderate temperature level (average  $330^\circ\text{C}$ ) with realistic discharge temperature of  $80^\circ\text{C}$  provides sufficient temperature differential for meaningful preheating applications. For air preheating from  $25^\circ\text{C}$  to  $200^\circ\text{C}$ , the required specific energy input is approximately 176 kJ/kg of air. This level is sufficient for meaningful fuel efficiency improvements in reheating furnaces.

### **Technical feasibility**

The off-gas ductwork from the billet preheating furnace offers accessible integration points for compact recuperators, and the relatively moderate flow rate (11.8 kg/s) permits economical recuperator sizing without excessive pressure drop penalties. The off-gas composition from billet preheating furnaces—predominantly  $\text{N}_2$ ,  $\text{CO}_2$ ,  $\text{H}_2\text{O}$ , and residual combustion products—is less aggressive than EAF primary off-gas, reducing fouling and corrosion risks and enabling the use of conventional stainless steel or lower-cost Inconel alloys for recuperator construction.

### **Future fuel compatibility**

Transition to hydrogen or biofuel combustion in the billet preheating furnace will alter exhaust gas mass amount, temperature and composition.

With respect to EAF off-gases, reheating furnace exhaust gas derives mainly from the fuel combustion; therefore, with hydrogen and at the same energy supplied, it is expected a higher mass reduction (e.g. between 15% and 20%), a higher temperature increase (still less than 5 %) and a higher increase of heat capacity (e.g. ranging from 10% to 12%) than in EAF off-gases.

Also in this case, both energy and exergy have been recalculated assuming the following variations of considered parameters:

- Mass reduction of 18% → **9.7 kg/s**
- Temperature increase of 4% → **260°C, 343°C, 478°C**
- Specific heat capacity increase of 11% → **1.33 kJ/(kg·K)**

With  $T_0 = 80^\circ\text{C}$ :

- 260°C → **2.3 MW** (sensible heat), **0.7 MW** (exergy)
- 343°C → **3.4 MW** (sensible heat), **1.3 MW** (exergy)
- 478°C → **5.1 MW** (sensible heat), **2.2 MW** (exergy)

For reference, with  $T_0 = 25^\circ\text{C}$  (theoretical):

- 260°C → **3.0 MW** (sensible heat), **0.8 MW** (exergy)
- 343°C → **4.1 MW** (sensible heat), **1.3 MW** (exergy)
- 478°C → **5.8 MW** (sensible heat), **2.3 MW** (exergy)

As expected, slightly higher changes are observed with respect to EAF off-gases; however, also in this case the variations of the parameters almost compensate each other even with realistic discharge temperatures.

The moderate temperature levels, also in case of foreseen increases (260–478°C), reduce material stress and corrosion risk compared to higher-temperature EAF off-gas applications.

### Priority 3: EAF Off-Gas After Quenching

#### *Thermal characterization*

**Flow:** same as Priority 1 (**46.6 kg/s**)

**Temperature:**  $\approx 250^\circ\text{C}$

#### *Energy/exergy evaluation*

For this source already at moderate temperature,  $T_0 = 80^\circ\text{C}$  is used as the realistic atmospheric discharge temperature:

- Sensible heat flow rate: **9.5 MW**
- Exergy flow rate: **3.0 MW**

For reference, with  $T_0 = 25^\circ\text{C}$  (theoretical):

- Sensible heat flow rate: **12.6 MW**
- Exergy flow rate: **3.2 MW**

The EAF off-gas downstream of the quenching system represents a tertiary-priority heat source suitable for lower-temperature preheating applications. The moderate

temperature (250°C) with realistic discharge to 80°C provides limited but meaningful temperature differential. Air preheating to 150–180°C is feasible with this source. While this preheating level provides meaningful fuel savings—typically 10–15% natural gas reduction in reheating furnaces—the efficiency improvement is lower than achievable with Priority 1 or Priority 2 sources. However, the substantial mass flow rate (46.6 kg/s) implies significant total thermal power availability, suggesting that this source could serve as a heat recovery source if filtration and dust removal of Priority 1 source (before quenching) prove economically unviable.

### **Technical feasibility**

Practical feasibility is enhanced relative to Priority 1 because the off-gas has already passed through the quenching system, resulting in reduced particulate loading and lower fouling risk for heat exchanger surfaces. This characteristic permits the use of compact, lower-cost recuperator designs with reduced maintenance requirements, improving economic viability despite the lower energy content.

### **Future fuel compatibility**

The moderate temperature and post-quenching location imply that this source will remain relatively stable in terms of temperature during transition to hydrogen or biofuel combustion, with mass amount and compositional changes (elevated H<sub>2</sub>O content in case of hydrogen) being the primary effects. Considering the same variations assumed in Priority 1, except for temperature, the following values for Sensible heat flow rate and Exergy flow rate have been obtained.

With  $T_0 = 80^\circ\text{C}$ :

- Sensible heat flow rate: **9.3 MW**
- Exergy flow rate: **2.9 MW**

For reference, with  $T_0 = 25^\circ\text{C}$  (theoretical):

- Sensible heat flow rate: **12.4 MW**
- Exergy flow rate: **3.2 MW**

Almost negligible changes are observed.

Conventional stainless steel or low-alloy recuperators are adequate for this application, reducing capital investment and facilitating rapid deployment.

## **Non-Prioritized Sources: EAF Secondary Off-Gas**

### **Thermal characterization**

**Flow:**  $\approx 1,200,000 \text{ Nm}^3/\text{h} \rightarrow 430 \text{ kg/s}$

**Temperature:** 55–100°C (average 78°C)

### **Energy/exergy evaluation**

A  $T_0 = 25^\circ\text{C}$  is used, assuming cooling to ambient temperature.

**Sensible heat flow rate:**

- 55°C → **15.5 MW**
- 78°C → **27.3 MW**
- 100°C → **38.7 MW**

**Exergy flow rate:**

- 55°C → **0.7 MW**
- 78°C → **2.2 MW**
- 100°C → **4.2 MW**

**Technical feasibility**

The EAF secondary off-gas, characterized by low temperature levels despite very high mass flow rates and for which no significant changes are expected by varying fuel in EAF-burners, is not prioritized for preheating strategies targeting reheating furnaces. While the sensible heat content represents substantial thermal power (27.3 MW at 78°C average), the exergy content is minimal (2.2 MW), reflecting the limited thermodynamic quality of this stream. Temperatures below 100°C are insufficient for meaningful air or fuel preheating in reheating furnace applications, where inlet temperatures typically range from 25 to 400°C and target preheating levels are 150–350°C. The exergy density is too low (thermodynamically “low-grade heat”).

This source is better suited for district heating networks, facility space heating, or process water preheating—applications that can effectively utilize low-temperature thermal energy without stringent temperature requirements. Such applications fall outside the scope of preheating strategies for downstream processes and are reserved for future phases focusing on site-level thermal integration.

The exclusion of this source from the prioritized list for preheating strategies does not diminish its value for overall site energy efficiency; rather, it reflects the cascading principle: reserve high-exergy streams for high-quality applications, and allocate low-exergy streams to appropriate sinks.

**Priority 4: Preheating of combustion fuel with EAF Off-gas**

Heat/exergy evaluation in accordance to previous priorities.

It becomes interesting with increasing amount of hydrogen in the fuel. The ratio fuel to combustion air increases and hence a use case is created to improve efficiency.

**Technical feasibility**

In general, every off-gas is suitable for preheating fuels. In analogy to the preheating of combustion air, with more (sensible) heat being available higher efficiency can be

achieved. The consideration of primary and secondary off-gas from the EAF might be governed by the requirements for safety when preheating hydrogen.

#### ***Future Fuel compatibility***

The compatibility is given, as one of the near future options for combustion might be the incorporation of ammonia. In combination with hydrogen from mixing, partial or thermal cracking might be the requirement for fuel preheating to preserve combustion efficiencies.

### **Priority 5: Heat pumps for warm water provision of local facilities**

Sensible heat flow rate and exergy flow rate are considered negligible in comparison to the previous entries. Nevertheless, the application to EAF Off-gas after quenching might be preferred since the high temperature heat sources should be used, among other areas, in fuel preheating.

#### ***Technical feasibility***

The temperatures at any point in the Off-gas are more than suitable for the application of heat pumps for residential applications. Eventually, the susceptibility to clogging when it comes to Off-gas must be investigated.

While high temperature off-gas is more profitable in preheating fuels, the heat pump usage can be predestined for the use with low-temperature off-gas.

#### ***Future Fuel compatibility***

The required temperature range for non-industrial heat pumps is entirely unaffected from the fuel mixtures.

## Summary of Priority Ranking

The prioritized hierarchy of heat sources for preheating strategies at FER, ranked by exergy content, technical feasibility, and future fuel compatibility, is summarized in Table

Priority Rank	Heat Source	Sensible heat flow rate [MW]	Exergy flow rate [MW]	Temperature Range [°C]	Application
1	EAF Off-Gas Before Quenching	11.2-30.8 11.4-31.1	5.3-17.9 5.5-18.2	400-750 408-765	Excellent for high-temperature air/fuel preheating
2	Roll Mill 2 Off-Gas from Billet Preheating	2.4-5.4 2.3-5.1	0.8-2.3 0.7-2.2	250-460 260-478	Suitable for moderate-temperature air preheating
3	EAF Off-Gas After Quenching	9.5 9.3	3.0 2.9	≈ 250°C	Suitable for lower-temperature air preheating or cascaded recovery
4	EAF Off-gas for fuel preheating	//	//	//	Fuel preheating
5	Heat Pump for warm water provision	//	//	//	District heating

green values in case of hydrogen as fuel

**Table 3: Ranking of FER heat sources**

Sources not prioritized for preheating strategies include EAF secondary off-gas (low temperature, more suitable for alternative applications such as district heating or process water preheating).

### 4.3 Acciaierie d'Italia Priority Sources

Based on the thermal mapping performed in Section 2.2 for the Acciaierie d'Italia (ADI) site, the identified heat sources have been prioritized. The selection logic prioritizes streams with higher thermodynamic quality (exergy) capable of improving process efficiency (e.g., maintaining material temperature to reduce upstream furnace load) over low-grade heat sources.

The analysis focuses on the hot strip mill area, specifically:

1. Radiant and convective heat losses during the transfer of the bar from the roughing mill to the finishing stand.
2. Radiant and convective heat losses during coil cooling from the down coiler to storage.
3. Thermal energy contained in the skid beam cooling water.

#### Priority 1: Heat losses during hot rolling

##### *Thermal characterization*

**Temperature:** The core temperature evolution of the bar head is shown in Figure 6.

- **Furnace Discharge:** Approximately **1,250 °C**.
- **Finishing Mill Exit:** The temperature drops significantly during the roughing and finishing process, reaching approximately **875 °C** at the end of the finishing mill.

**Specific Energy Loss:** The analysis in Section 2.2 indicates that the most significant specific thermal loss occurs during the transfer after the sixth roughing stand (R6), quantified at approximately **64 kJ/kg**.

**Estimated Power:** Assuming a standard reference productivity for a hot strip mill of this class at 300 tons/hour (83.3 kg/s):  $\text{Power} = 64 \text{ kJ/kg} * 83.3 \text{ kg/s} =$  approximately **5.3 MW**.

##### *Energy/exergy evaluation*

**Sensible heat flow rate:** Approximately 5.3 MW (estimated based on specific losses).

**Exergy flow rate:** High. With source temperatures exceeding 1,000°C, the thermodynamic quality is exceptional.

##### *Technical feasibility*

The recovery strategy for this source does not involve a traditional heat exchanger but rather the mitigation of losses (passive/active panels). Capturing this energy implies preventing its dissipation. The technical feasibility relies on the installation of insulating covers or active heating shields between the roughing and finishing stands. This aligns with the objectives of WP3 regarding “Hot Charging” and process efficiency. The primary challenge is mechanical integration with the roller table and ensuring maintenance access.

### *Future fuel compatibility*

This priority is fuel-neutral but critical for the transition to hydrogen. By reducing thermal losses by about 64 kJ/kg, the required discharge temperature from the reheating furnace can be lowered, or the heating curve optimized. This directly reduces the specific consumption of high-value future fuels (Hydrogen) in the reheating furnace.

## **Priority 2: Radiant heat from coil cooling (down coiler to storage)**

### *Thermal characterization*

**Temperature:** According to the updated simulation of 4 representative coils (Table 2), the temperature evolution over **3 hours** shows distinct behaviours for core and surface:

- **Core:** The core temperature decreases by more than 250°C, dropping from the coiling temperature (range 550–700°C) to lower values.
- **Surface:** The surface temperature drops rapidly, reaching values near 230°C after 3 hours.

**Mass Estimation:** Based on the dimensions of the 4 simulated coils (Table 2), the mass varies significantly:

- **Density of steel:** 7850 kg/m<sup>3</sup>.
- **Assumed Inner Diameter:** ≈ 760 mm (typical mandrel size).
- **Volume Range:** 2.11 m<sup>3</sup> (Coil 1) to 4.57 m<sup>3</sup> (Coil 3)
- **Mass Range:** 16.6 tons (Coil 1) to 35.9 tons (Coil 3).
- **Average Mass:** ≈25.3 tons

**Estimated Power:** Calculating the sensible heat loss for a core temperature drop of 250 °C over 3 hours (so, the additional temperature drop at the surface is conservatively neglected):

- **Energy Released per Coil:** Ranges from **2.0 GJ** (Coil 1) to **4.4 GJ** (Coil 3).
- **Average Thermal Power per Coil:** Ranging from **188** to **407 kW** (depending on coil size).
- **Site Potential:** For instance, for a storage bay with **40** active coils, the total available power would be **>10 MW**.

### *Energy/exergy evaluation*

**Sensible heat flow rate:** High aggregate potential (multi-megawatt scale depending on storage logistics).

**Exergy flow rate:** Medium. While the total energy is high, the rapid surface cooling to ≈230°C reduces the grade of heat available for immediate radiative recovery, reinforcing the need for insulation to preserve the higher-grade core heat.

### *Technical feasibility*

While recovering this heat via air-to-air heat exchangers (hoods over storage areas) is technically feasible, it is logistically complex due to crane movements. An alternative could be the use of a thermal tunnel, consisting of heat exchangers, where the coils pass up to the conveyor (from the downcoiler to the transfer table). This would allow for a continuous flow of strips from the coil storage areas (not all are stored in the same place but can be transferred for subsequent maritime or rail transport) with a higher exchange rate. In fact, the reduction in surface temperature is greater during the transfer of the coils at the entrance of the conveyors (Figure 10).

### *Future fuel compatibility*

Similar to Priority 1, preserving coil heat reduces the energy demand for downstream annealing or reheating processes, directly reducing the consumption of Hydrogen or electricity required for those steps.

## **Priority 3: Skid beam cooling systems**

### *Thermal characterization*

**Flow Rate:** Furnaces 1, 2, and 3 operate at approximately 2,500 m<sup>3</sup>/h per furnace. Furnaces 4 and 5 operate at approximately 500 m<sup>3</sup>/h per furnace.

### **Temperature:**

- Furnaces 1–3: Temperature difference is approximately 5 °C. Figure 12 shows inlet temperatures around 25 °C and outlet temperatures around 30–32 °C.
- Furnaces 4–5: Temperature difference is approximately 20 °C. Assuming similar inlet conditions, outlet temperatures would be approx. 45 °C.
- Overall Range: The fluid temperature is very low, typically 25–45 °C.

**Thermal Power:** Data collected for Furnace 1 indicates energy losses ranging 11.2 to 14.5 MW. The total site potential across five furnaces is therefore extremely high (>50 MW).

### *Energy/exergy evaluation*

**Sensible heat flow rate:** Very High (>15 MW per furnace for the large units).

**Exergy flow rate:** Very Low. The energy is contained in water at temperatures (25–45 °C) that are barely above ambient, severely limiting its capacity to do useful work.

### *Technical feasibility*

Technically, feasibility for capture is very high as the energy is already contained in a fluid circuit. However, the application is limited by the low temperature. It is not suitable for preheating combustion air or fuel for the furnaces. It is suitable for district heating and internal process water heating.

### Future fuel compatibility

This source is independent of the fuel type used in the furnace. It represents a baseload waste heat source. Due to its low exergy, it is ranked lower than the rolling/coil sources for the specific objectives of process-integrated preheating, though it remains vital for general plant efficiency.

### Summary of Priority Ranking

The prioritized hierarchy of heat sources for ADI, focused on supporting the decarbonization of the reheating and rolling process, is summarized in Table 4.

Priority Rank	Heat Source	Sensible heat flow rate (MW)	Exergy flow rate (MW)	Temperature Range	Application
1	Hot Rolling Transfer Bar (R6-F1)	~5.3 (estimated)	High	1,050–1,250°C	Avoided energy loss (active/passive panels) to reduce furnace fuel
2	Coil Cooling (Storage)	>10 (aggregate)	Medium/High	380–600°C	Thermal tunnel with heat exchangers
3	Skid Beam Cooling (Furnace 1)	11.2–14.5	Low	25–45°C	District heating / process water preheating

**Table 4: Ranking of ADI heat sources**

## 5. Conclusions and recommendations

The short-term heat recovery analysis carried out in **E-ECO Downstream** has successfully mapped and characterized the residual energy flows at the Feralpi Siderurgica (FER) and Acciaierie d'Italia (ADI) industrial sites. By applying thermodynamic principles of exergy and sensible heat, the consortium has prioritized heat sources that offer the highest potential for immediate decarbonization and energy efficiency improvements.

### Key Findings:

1. The analysis confirms that thermal power alone is a poor indicator of recovery potential. At **FER**, the Secondary Off-Gas system contains massive thermal power but negligible exergy flow rate, rendering it unsuitable for high-grade processes. Conversely, the **EAF Primary Off-Gas (pre-quenching)** offers high-quality heat capable of driving significant air or fuel preheating.
2. **Site-Specific Opportunities:**
  - **At FER**, the priority is the interception of EAF off-gases before the quenching tower. This “high-grade” source is the optimal candidate for the testing of the new corrosion-resistant recuperator designs developed in WP2.
  - **At ADI**, the highest potential lies in “avoided losses” rather than downstream recovery. The significant exergy destruction observed during the transfer bar movement and coil cooling strongly supports the **Hot Charging** strategy (WP3) using active/passive covers to retain high temperatures for downstream processes.
3. The transition to hydrogen combustion will alter the thermal landscape. The analysis predicts that while the thermal power of off-gases may remain stable, the **moisture content will rise drastically**, increasing the dew point and the specific heat capacity. This validates the project's focus on developing advanced Ni-based alloys (WP1) for recuperators that must withstand Hydrogen-Induced Stress Corrosion Cracking (HISCC) in humid, high-temperature environments.

### Recommendations:

- **Pilot Testing (WP2):** Proceed with the design of the pilot recuperator targeting the specific conditions of the FER EAF primary off-gas ensuring materials are tested against the corrosion profiles of H<sub>2</sub>-rich exhaust.
- **Hot Charging Implementation (WP3):** Focus simulation efforts on the mechanical integration of insulating covers at ADI, as preserving the temperature of the transfer bar yields a higher net energy benefit than attempting to recover that energy later from low-grade cooling water.

- **Low-Grade Heat:** While Skid Beam cooling (ADI) and Secondary Off-Gas (FER) are deprioritized, they remain assets for district heating in the medium-long term roadmap (WP5).

The results and inventory of heat sources generated in this analysis (Task 2.1) are hereby passed to Task 2.2 to serve as the functional baseline for the selection of the most suitable recovery systems and the calculation of potential energy savings. This analysis provides the boundary conditions necessary for the detailed engineering of the heat recovery prototypes and defines the baseline for the LCA and economic assessments to follow.